International Journal of Solids and Structures 50 (2013) 2980–2994

Contents lists available at SciVerse ScienceDirect

International Journal of Solids and Structures

journal homepage: www.elsevier.com/locate/ijsolstr

Structural behavior of solid expandable tubular undergoes radial expansion process – Analytical, numerical, and experimental approaches

Omar S. Al-Abri *, Tasneem Pervez

Department of Mechanical and Industrial Engineering, College of Engineering, Sultan Qaboos University, P.O. Box 33, Al-Khoud 123, Oman

ARTICLE INFO

Article history:
Received 3 January 2013
Received in revised form 31 March 2013
Available online 28 May 2013

Keywords:
Steel
Finite element method
Metal forming
Solid Expandable Tubular Technology
Thick-wall tube
Tube expansion
Well drilling

ABSTRACT

Today's structures have to meet increasingly rigorous requirements during operation. The economic and human costs of failure during service impose a great responsibility on organizations and individuals who develop new products as well as those who select/integrate products in a final engineering design. A crucial aspect for successful product development and/or inclusion is the careful selection of the best material(s), derived from an informed awareness of the capabilities and opportunities afforded by all candidate materials, together with a design that takes full benefit of those competencies. Thick-wall tubular is an example where all these issues are playing a major role in deciding their industrial applications. Given for their desirable features of high strength and geometrical shape, they are widely used in aerospace, marine, military, automotive, oil and gas, and many other fields. This paper focuses on developing analytical solution to investigate the structural response of thick-wall tubulars undergo plastic deformation due to expanding them using a rigid mandrel of conical shape. Volume incompressible condition together with the Levy–Mises flow rule were used to develop the equations which relate the expansion ratio of the tubular to the length and thickness variations. Besides, Tresca's yield criterion was used to include the plastic behavior of the tubular material. Further to this, a numerical model of the tubular expansion process was also developed using the commercial finite element software ABAQUS. Experiments of tubular expansion have been conducted using a full-scale test-rig in the Engineering Research Laboratory at Sultan Qaboos University to validate the analytical and numerical solutions. The developed analytical and numerical models are capable of predicting the stress field in the expansion zone, the force required for expansion, as well as the length and thickness variations induced in the tubular due to the expansion process. Comparison between analytical, experimental, and simulation results showed that a good agreement has been attained for various parameters.

1. Introduction

The continuously increasing demands for petroleum products have forced the petroleum companies from all around the world to search for new reservoirs or to revitalize the existing ones, which are difficult to access and/or maintain a profitable production level. Current well drilling and operation technologies cannot provide cost effective solutions for emerging challenges in this field. The well-bore tubular technology has gained significant importance in every well with maturation in oil and gas industry. The conventional well-bore tubular technology has progressed over decades of research work including laboratory experiments and field trials that produced satisfactory results. Currently, telescoping of well size, from wellhead down to the reservoir, is a result of conventional well construction methods. This ends up in high cost of surface casing, wellheads and operating equipments. At times, the method also results in an unworkable small hole size at the target depth. This could lead to unprofitable production or in worst cases failure to reach the desired target. The conventional well-bore tubular technology is still unable to provide solutions for many problems such as deep drilling, conservation of hole size during hydraulic isolation processes, and accessing of new reservoirs that currently cannot be reached economically. These issues as well as many others are not only long-standing but have far-reaching consequences in the oil and gas industry. They involve one of the industry's most fundamental technologies: well-bore tubulars. The revolutionary new Solid Expandable Tubular (SET) Technology has successfully addressed some of the above-mentioned issues. It provides mechanical stability in situations where conventional casing strings cannot be installed due to geometrical restrictions. Further to this, larger diameters can be attained at terminal depths for enhanced production from a single well. Thus, it has gained momentum and attracted the attention of operators and researchers, and is rapidly expanding its horizon of applications.

* Corresponding author. Tel.: +968 2414 2652; fax: +968 2414 1316.
E-mail address: m053898@squ.edu.om (O.S. Al-Abri).

0020-7683/$ - see front matter © 2013 Elsevier Ltd. All rights reserved.
http://dx.doi.org/10.1016/j.ijsolstr.2013.05.013

Nomenclature

μ	coefficient of friction	t_2	final tubular thickness (m)
F_e	expansion force (N)	Y	tensile yield strength (Pa)
m	correction factor that may be taken between 1 and 1.15 to approximate the von Mises yield criterion	z	instantaneous tubular length (m)
		z_1	initial tubular length (m)
P_c	contact pressure between mandrel and tubular	z_2	final tubular length (m)
r	instantaneous tubular radius along the expansion zone	α	mandrel cone angle (°)
r_{i1}	pre-expansion tubular inner radius (m)	β	$90° - \alpha$
r_{o1}	pre-expansion tubular outer radius (m)	$\sigma_{z/r/t}$	axial, radial, or hoop stress (Pa)
r_{i2}	post-expansion tubular inner radius (m)	σ_e	equivalent stress (Pa)
r_{o2}	post-expansion tubular outer radius (m)	OD	outer diameter
t	instantaneous tubular thickness (m)	P_{cr}	collapse pressure rating
t_1	initial tubular thickness (m)	P_{Yi}	internal pressure rating at the onset of yielding

The notion of using this technology in the oil and gas industry started to take place in the late 1990s, driven by operators' aspiration to trim down the telescopic effect in casings design as the wells are drilled deeper. The basic idea was studied in several papers published during the last decade. The concept of SET Technology is simple to understand and consists of a down-hole in situ expansion of the tubular inner diameter that is attained by hydraulic and/or mechanical forces to pull/push a solid mandrel from the bottom up that permanently deforms the tubular to the required size as shown in Fig. 1. Since then, the technology has continued to grow in acceptance and use, where in a period of two years, the reliability of the technology has improved from an average of 67% in 2000 to over 95% in 2002 (Escobar et al., 2003). This has lead to the development of a collection of products that can be utilized as solutions for an ample range of drilling, completion, and production problems. Many different designs and processes have been created over the years, and as the oil industry continues to grow and change, expandables are also evolving to generate new and innovative solutions to the ever-shifting issues that operators' deal with. The ultimate goal is to realize the drilling of slim to mono-diameter oil and gas wells as opposed to the current practices of drilling telescopic wells as shown in Fig. 2. Reducing the telescopic nature of the conventional wells would allow a much smaller surface casing to be used and subsequent casings could be reduced in diameter. Additionally, with the aid of this technology, operators will be able to reduce the amount of resources required to construct the well, as well as reaching target depths with bigger diameter. Several economic evaluations have been performed to show the cost effectiveness of this new technology (Owoeye et al., 2000; Benzie et al., 2000; Dupal et al., 2001). Through field trials and case studies Dupal et al. (2001), Gusevik and Merritt (2002) and other researchers (Benzie et al., 2000) showed that open-hole solid expandable tubular have the potential to reduce the overall well construction cost. An interesting case was reported in Campo et al. (2003) showed that the mono-diameter system provides 48% cost reduction in well construction as compared to the fifth generation drillship cost and 33% cost reduction when compared with high specification semisubmersible. The environmental benefits are also substantial. Campo et al. (2003) reported a remarkable environmental impact of solid expandable tubular due to lesser requirement of consumables for well construction. The study showed 44% reduction in drilling fluid volume, 42% in cement volume and 42% in casing tonnage. These environmental impacts prove that the energy industry can fulfill world's demand for hydrocarbon products with an environmentally friendly process.

Much of the activities accompanying the introduction of SET Technology in petroleum industry were related to the effect of the expansion process on the material properties (Filippov et al., 1999; Mack et al., 1999; Stewart et al., 1999; Mack et al., 2000). Solid tubulars having adequate material properties characterized by collapse and burst strength, ductility, impact toughness, resistance to wear and environmental cracking must be carefully selected for down-hole applications. An API Grade L-80 expandable steel tubular of 5–1/2 in diameter was tested to determine the effect of expansion on the mechanical properties (Filippov et al., 1999; Mack et al., 1999). The results showed that the ultimate tensile strength increases, the elongation tends to decrease and the collapse rating decreases. The test data reveal no detrimental effect

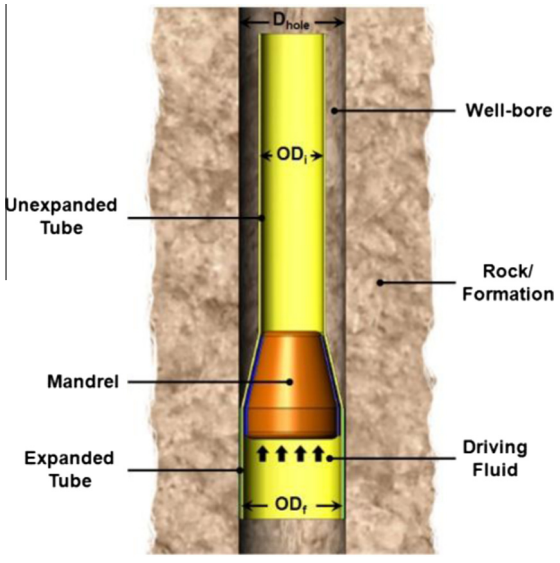

Fig. 1. Schematic diagram of tubular expansion process using conical mandrel.

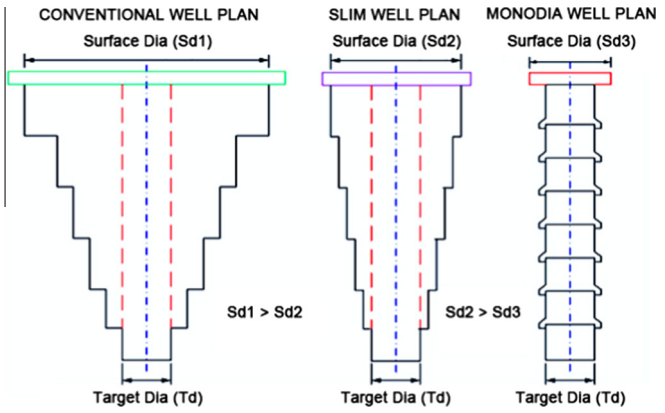

Fig. 2. Schematic sketch of conventional to mono-diameter oil-wells.

on burst strength. Benzie et al. (2000) and Ruggier et al. (2001) attributed the decrease in collapse pressure to the length and thickness variation, Bauschinger effect, and residual stresses. The expansion process does not affect burst pressure because the plastic work during expansion, which increases the strength of tubular; compensate the losses in wall thickness (Dupal et al. 2001). Klever and Stewart (1998) and Stewart and Klever (1998) developed a mathematical model which describes the effects of irregularities on the burst strength of the subjected tubular. Later, Stewart et al. (1999) extended the mathematical model to solid expandable tubular and conducted a laboratory test at Aachen University of Technology using a 3–1/2 in (OD) Grade B tubular following X42 ASTM A106 standards. The results showed that the yield strength increases in the order of 70% and the ultimate tensile strength increases in the order of 30%, whereas the elongation at fracture decreases in the order of 50% and the uniform strain decreases from 19.4% to 1.4%. Enventure Global Technology performed the first commercial application of Solid Expandable Tubular Technology in November 1999. The results of this successful expansion showed a decrease of 4.2% in length, a minor reduction as well in wall thickness and a reduction of 50% in collapse pressure (Mack et al., 2000). Much less effect on the burst pressure is observed.

In Oman, the research on expandable tubing technology started lately with the support from the local oil companies. This is due to the need to know how to best adopt expandable tubular applications for well drilling and remediation in the Sultanate. The goals are to produce from difficult reservoirs, increase oil production, reduce unwanted production of water, and lower the cost of expandable tubular technology. However, oil recovery in Omani reservoirs is often impaired by zones of high permeability i.e., fractures, fault-related fracture corridors, karstied parts of the reservoir, etc. (Fokker et al., 2005; Lighthelm et al., 2006; Marketz et al., 2005; Ozkaya and Richard, 2006) which can span from an aquifer to the wellbore. Several carbonate aquifers in Oman have been developed by horizontal wells, which are often intersected by these fractures, resulting in severe losses. Drilling through fractured reservoir sections causes drilling losses that have to be cured to be able to place cement in the annulus. As well, fractures may become potential avenues for the injected water to bypass large volumes of oil resulting in a poor sweep efficiency of the conventional water flooding operations and thus the water is cycled without any improvement in oil production (Chilingraian et al., 1996). In order to avoid this shortcut between the aquifer-formation interfaces (initial oil–water contact), hydro-isolation is usually carried out by cementing, chemical treatment, and installation of scab liners in the vicinity of the wellbore-fracture intersections. However, these mechanical and chemical techniques implemented in fractured carbonate reservoirs in a series of wells had limited success owing to drilling losses, high cost of gels, intensive seepage around the short seal of external casing packers, etc. (Al-Dhafeeri and Nasr-El-Din, 2007). Therefore, expandable tubular and swelling elastomer sealing technologies have been introduced for wells drilling as an alternative to cemented liners. This is done to provide zonal isolation which is critical for profile control, eliminate the need for curing losses and liner cementation, and slim down the well design, i.e., reduce the size of the top hole to reduce footprints. This non-invasive or invasive technique, depending on the use of elastomers, is applied in several wells with water rates reduction up to 40% and oil gains up to 45 m^3 per day per well (Welling et al., 2007). Nevertheless, still a lot of issues need to be resolved before this technology can be used to its full potential for well drilling and remediation. In this contest, the research in Oman at the early stages was focused on developing semi-analytical and finite element models that address different issues of this emerging technology. However, the capacity of the research has been strengthened with the inauguration of the expandable tubular test-rig at Sultan Qaboos University (SQU) in 2009 which has helped local operators to use this technology with confidence. The research activities tackled many essential issues including: simulation of tubular expansion in well drilling using nonlinear explicit finite element method to study the effect of different expansion ratios, friction coefficients and mandrel angles on the tubular expansion process (Pervez et al., 2005), simplified mathematical model for tubular expansion process (Seibi et al., 2005), analytical solution for wave propagation due to pop-out phenomenon (Seibi et al., 2006), post-expansion tube response under mechanical and hydraulic expansion – a comparative study (Seibi et al., 2007), research on possibility of using aluminum as expandable tubular instead of steel (Pervez et al., 2008), dynamic effects of mandrel–tubular interaction in down-hole tubular expansion process (Seibi et al., 2009), experimental and numerical investigation of expandable tubular structural integrity for well applications (Pervez 2010; Pervez et al., 2012b), simulation of tubular expansion in irregularly shaped boreholes (Pervez et al., 2011), and finite element analysis of tubular ovality in oil wells (Pervez and Qamar, 2011). The results showed that tubular wall thickness decreases with an increase in mandrel angle, expansion ratio, and friction coefficient. In addition, the tubular length often shortens for expansion under tension for most of the loading mechanisms. However, it elongates at high friction levels due to the resistance that opposes the interface materials from flowing smoothly over each other creating some tension in the tubular.

Developing a mathematical model that represents the tubular expansion process is a powerful tool that would help in alleviating the need for conducting the costly experiments or even the time consuming simulation practices via the finite element method. With a set of mathematical equations, a program that could help field engineers in amassing data on the expandable tubular technology could be created which would helps in reducing time with regard to the experimental and simulation practices, and brings down the effort and cost involved. A review of selected literature on developing analytical solution for thick-wall tubulars revealed the availability of many papers that attempted to study the elastic–plastic behavior of thick-wall cylindrical shells subjected to different types of loading (Hausenbauer and Lee, 1966; Perry and Aboudi, 2003; Gao, 2003; Ayob et al., 2009; Darijani et al., 2009). However, there are only a few studies dealing with the plastic deformation of thick cylindrical shells, and even fewer studies that deal with the behavior of these structures under plastic deformation due to expanding them using a mandrel. Recently, plasticity and membrane theories were used to develop analytical models for expansion of thin-walled tubulars with a conical expansion tool (Al-Hiddabi et al., 2002; Ruan and Maurer, 2005). The models demonstrate the variation in the force required for expansion with respect to expansion ratio, friction coefficient, mandrel geometry, and tubular material's yield strength. Karrech and Seibi (2010) developed a model to predict the stress field in the expanded zone and the dissipated energy due to the expansion process. However, when the cylinder has an inner-radius-to-wall-thickness ratio of less than 10, thin-walled cylinder equations are no longer hold since stresses vary significantly between inside and outside surfaces and shear stress through the cross section can no longer be neglected. Thus, the need for the current work, which focuses on developing analytical solution for thick-walled solid expandable tubular subjected to large plastic deformations (where the tubular expands up to 30% of its original inner diameter).

The paper is divided into six major sections. Section 2 includes the mathematical formulations of the developed analytical model. Development of a finite element model of the tubular expansion process is presented in Section 3, followed by a description of the experimental work is discussed in Section 4. Section 5 consists of the results and discussion part, followed by the conclusions in Section 6.

2. Analytical modelling

Propagating a mandrel of conical shape through a tube of a certain wall thickness is considered in this study as shown in Fig. 3. As the mandrel moves through the tube, each part of the tube passes through exactly the same process, and if the tube is sufficiently long, a steady-state condition is attained. Governing equations are derived based on the equilibrium and incompressibility conditions of a conical ring element that has been selected from the inside material of the tubular wall being expanded to account for the stress variations according to the Saint–Venant's principle. The free body diagram of the conical ring subjected to tangential and radial stresses is shown in Fig. 4.

Now, it is important to clarify that cylinders are classified as being either open – in which there is no axial component of wall stress, or closed – in which an axial stress must exist to equilibrate the fluid pressure. In the current study which is related to perform a radial expansion of a tube using a conical mandrel that is propagated inside the tubular utilizing a differential pressure, the procedure usually adopted in performing this operation in down-hole is to place the tube in the location of interest and then perform the expansion process. The installed tubular is usually provided with a canister that works as pressure chamber to accumulate the pressure that will push the mandrel forward. This canister is usually consists of a shoe that is placed at the bottom end of the tube and works as an end-cap while the mandrel works as the front-cap. In this process, usually one of the ends of the tubular is kept un-restrained deliberately to allow free length change that is required to compensate the increase in diameter in accordance with the volume conservation condition otherwise a severe reduction in thickness will be confronted if both ends of the tubular are restrained.

Now, to model this scenario, if a plane strain (i.e., $\varepsilon_z = 0$) is considered, then it means that the tubular is restrained between rigid supports (i.e., negligible change in length). Whereas, the current situation is more of being a cylinder with caps that is free to change its length. But, in order to handle this situation, it is difficult to get a direct solution by considering all the stresses at the same time. Therefore, the procedure to be adopted over here is to consider an open-end cylinder for which the hoop and radial stresses are exists, and then move to the closed-end cylinder to obtain the axial stress from the statics equilibrium, while assuming that the hoop and radial stresses in a closed-end cylinder are the same as for an open-ended cylinder (Hausenbauer and Lee, 1966).

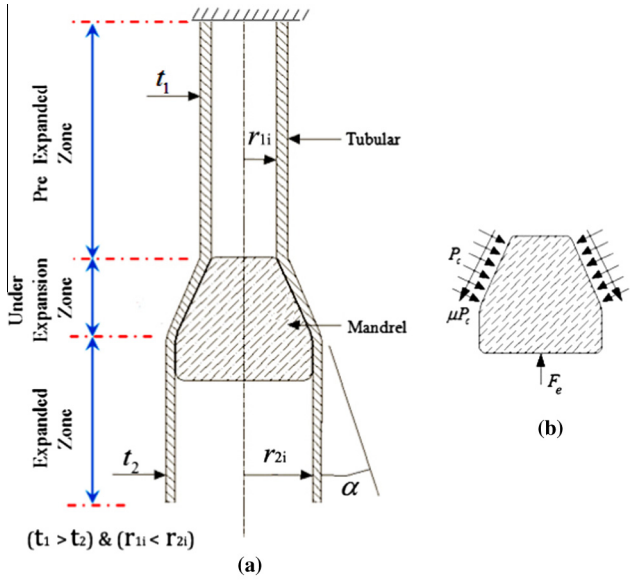

Fig. 3. Schematic diagram of a mandrel–tubular system: (a) free-body diagram of a tubular under compression expansion; (b) free-body diagram of the mandrel.

Thus, the principle stresses in a thick-wall closed-end cylinder are such that the hoop and radial stresses are based on a condition of plane stress in an open-ended cylinder while the axial stress is found from simple statics equilibrium for the closed-end cylinder. This is of course based on the assumption that the longitudinal stress is a form of membrane stress in that there is no variation across the thickness of the cylinder. This is the approach to be adopted in this investigation.

2.1. Assumptions

To simplify the problem and develop a mathematical model that can be solved with reasonable accuracy, the following assumptions have been made in order to obtain a solution for the expansion force and the variations in the tubular length and thickness due to the expansion process:

1. The only loadings act on the tubular are the contact pressure and the friction force that acts at the mandrel–tubular interface
2. The angle of the lateral side with the horizontal plane (β) is greater than 60° so that the influence of the shear forces is negligible.
3. The tube is in a state of plane stress with the axial stress ($\sigma_z = 0$) for the purpose of deriving the radial (σ_r) and the hoop (σ_t) stresses. Then, the longitudinal stress (σ_z) is obtained from the statics of the mandrel–tubular system while assuming that the hoop and radial stresses in a closed-end cylinder are the same as for an open-ended cylinder (Hausenbauer and Lee, 1966).

2.2. Equilibrium equations

From the free body diagram of the conical ring shown in Fig. 4(b), the projection of the areas of the inner and the outer surfaces are nothing except trapezoidal areas as shown in Fig. 4(c) and (d), and they can be estimated as:

$$\text{Inner trapezoidal area} = \left(\frac{1}{2}\text{altitude}\right) \times (\text{sum of bases}) = \frac{1}{2}(\sin(\beta)dy) \times (2r\sin(\beta) + 2r\sin(\beta) + 2\cos(\beta)dy) \quad (1)$$

$$\text{Outer trapezoidal area} = \left(\frac{1}{2}\sin(\beta)dy\right) \times [2(r\sin(\beta) + dr\sin(\beta)) + 2(r\sin(\beta) + dr\sin(\beta) + \cos(\beta)dy)] \quad (2)$$

Summation of the forces in the radial direction gives:

$$2\sigma_t(dydr) = -\sigma_r\left(\frac{dy}{2}(4r\sin^2(\beta) + 2\cos(\beta)\sin(\beta)dy)\right) + (\sigma_r + d\sigma_r) \times \left(\frac{dy}{2}\left(2r\sin^2(\beta) + 2dr\sin^2(\beta) + 2r\sin^2(\beta) + 2dr\sin^2(\beta) + 2\cos(\beta)\sin(\beta)dy\right)\right) \quad (3)$$

Simplifying the previous relation and neglecting the higher-order small terms yields:

$$\left(\frac{d\sigma_r}{dr}\right)r\sin^2(\beta) + \sigma_r\sin^2(\beta) - \sigma_t = 0 \quad (4)$$

Since the tubular experiences large plastic deformation, a relationship between the hoop (σ_t) and radial (σ_r) stresses can be established. In this case, Tresca's criterion is used and is defined, for zero axial stress, by:

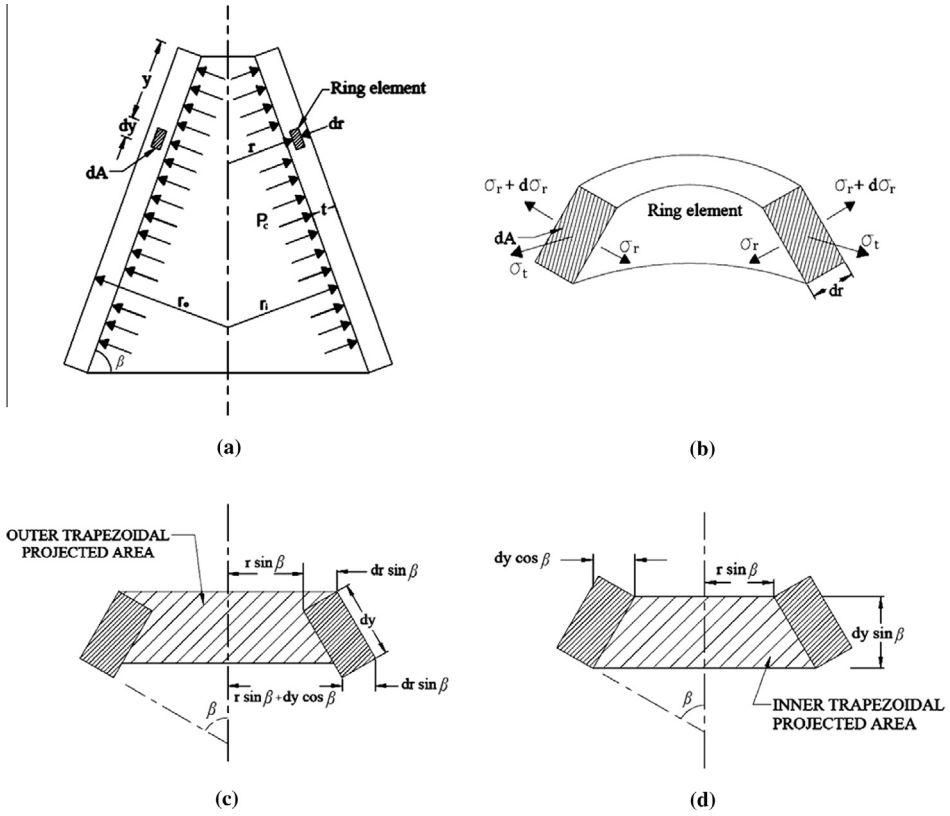

Fig. 4. (a) Free-body diagram of the under-expansion zone; (b) free-body diagram a conical tubular ring taken from inside the tubular wall; (c) projection of the outer surface area of the ring element; (d) projection of the inner surface area of the ring element.

$$\sigma_t - \sigma_r = mY \tag{5}$$

where Y is the tensile yield strength of the tubular material and m is a correction factor that may be taken between 1 and 1.15 to approximate the von Mises yield criterion (Chakrabarty, 2006). Substitutions of the hoop stress from Eq. (5) into Eq. (4) and rearrange the resulting equation yields the following relationship:

$$\frac{d\sigma_r}{\left(1-\sin^2(\beta)\right)\sigma_r + mY} = \frac{dr}{r\sin^2(\beta)} \tag{6}$$

Knowing that the only loadings act on the tubular are the contact pressure that acts at the mandrel/tubular interface yields a set of boundary conditions given by:

$$@(r = r_{1i}) \text{ and } (r = r_{2i}) \Rightarrow \sigma_r(r) = -P_c \tag{7-a}$$

$$@(r = r_{1o}) \text{ and } (r = r_{2o}) \Rightarrow \sigma_r(r) = 0 \tag{7-b}$$

where the subscripts i and o stand for the inner and outer surfaces, respectively, while the subscripts 1 and 2 denote the tubular radius in pre and post expansion phases. Now, using these boundary conditions, Eq. (6) can be integrated as following:

$$\int_{-P_c}^{0} \frac{d\sigma_r}{\left(1-\sin^2(\beta)\right)\sigma_r + mY} = \int_{r_{1i}}^{r_{1o}} \frac{dr}{r\sin^2(\beta)} \tag{8}$$

It is important to emphasize that the integration of Eq. (8) has been taken at (or close by) the un-expanded side. However, the integration limits can be taken at any other location as long as the values of those limits are known. For example, the boundary conditions specified by Eq. (7) are both valid. But, the un-expanded parameters (i.e., r_{1i} and r_{1o}) have been selected because their values are known from the tubular geometry while the other limits which represent the post-expansion properties (i.e., r_{2i} and r_{2o}) are not known because some thickness variation is expected to take place due to the expansion process. Thus, what would be the real outer radius after expansion (r_{2o}) is not known and thus it is not possible to use it.

After some mathematical manipulation, a relationship for the contact pressure (P_c) can be obtained as:

$$P_c = \frac{mY}{\left(\sin^2(\beta)-1\right)}\left(\left(\frac{r_{1o}}{r_{1i}}\right)^{\frac{\left(\sin^2(\beta)-1\right)}{\sin^2(\beta)}} - 1\right) \tag{9}$$

It is vital to note that the contact pressure (P_c) given by Eq. (9) is constant over the mandrel length because it is not function of the axial position along the mandrel. Rather, it depends on the tubular material (i.e., yield strength) and geometrical properties (i.e., r_{1i} and r_{1o}) as well as the amount of expansion ratio prescribed (i.e., the angle β). In reality, there is no doubt that the contact pressure is function of the axial position along the mandrel and this observation was very obvious from the author's previous investigation performed using finite element method and presented in (Pervez et al., 2012a). However, due to the complex behavior that has been observed and due to the lack of an expression that can be used to incorporate such behavior, the authors considered a uniform contact pressure in the current study just for the sake of simplicity. Impeding an expression of P_c that describes the non-uniform behavior can be done easily in the future just by replacing P_c in the current model with the new expression.

A relation between the external applied force (F_e) and the contact pressure at the mandrel/tubular interface (P_c) can be obtained

by considering the equilibrium of the mandrel, shown in Fig. 3(b), as:

$$F_e = \pi(r_{2i}^2 - r_{1i}^2)(1 + \mu\cot(\alpha))P_c \tag{10}$$

Now, combining Eqs. (9) and (10) one may obtain the following formula for the expansion force:

$$F_e = \pi(r_{2i}^2 - r_{1i}^2)(1 + \mu\cot(\alpha)) \times \frac{mY}{\left(\sin^2(\beta) - 1\right)}\left(\left(\frac{r_{1o}}{r_{1i}}\right)^{\frac{\sin^2(\beta)-1}{\sin^2(\beta)}} - 1\right) \tag{11}$$

A relationship for the longitudinal stress (σ_z) can be established from the statics of the mandrel–tubular system by assuming that the tubular is expanded under compression, hence at any point in the tubular located at the front end of the mandrel (i.e., $r = r_{1i}$ and $t = t_1$) we have:

$$\sigma_z = \frac{F_e}{\pi(r_{1o}^2 - r_{1i}^2)} \tag{12}$$

Now, combining Eqs. (11) and (12) yields:

$$\sigma_z = \frac{\pi(r_{2i}^2 - r_{1i}^2)(1 + \mu\cot(\alpha))}{\pi(r_{1o}^2 - r_{1i}^2)} \times \frac{mY}{\sin^2(\beta) - 1}\left(\left(\frac{r_{1o}}{r_{1i}}\right)^{\frac{\sin^2(\beta)-1}{\sin^2(\beta)}} - 1\right) \tag{13}$$

For thick-wall cylinders, stresses vary significantly between the inside and the outside surfaces, and the shear stress through the cross section cannot be neglected. Thus, a relation for the radial stress variations along the tubular thickness can be obtained using the following boundary conditions:

$$@(r = r_{1i}) \Rightarrow \sigma_r(r) = -P_c \tag{14-a}$$

$$@(r = r) \Rightarrow \sigma_r(r) = \sigma_r \tag{14-b}$$

Using these boundary conditions, Eq. (6) can be integrated as following:

$$\int_{-P_c}^{\sigma_r} \frac{d\sigma_r}{\left(1 - \sin^2(\beta)\right)\sigma_r + mY} = \int_{r_{1i}}^{r} \frac{dr}{r\sin^2(\beta)} \tag{15}$$

After some mathematical manipulation, a relationship for the radial stress at any radial position can be obtained as:

$$\sigma_r = \left(\frac{\left(\sin^2(\beta) - 1\right)P_c + mY}{1 - \sin^2(\beta)}\right)\left(\frac{r}{r_{1i}}\right)^{\frac{\left(1-\sin^2(\beta)\right)}{\sin^2(\beta)}} - \frac{mY}{1 - \sin^2(\beta)} \tag{16}$$

Substituting for P_c from Eq. (9) and simplifying the formula yields:

$$\sigma_r = \frac{mY}{1 - \sin^2(\beta)}\left(\left(\frac{r_{1o}}{r_{1i}}\right)^{\frac{\left(\sin^2(\beta)-1\right)}{\sin^2(\beta)}}\left(\frac{r}{r_{1i}}\right)^{\frac{(1-\sin^2(\beta))}{\sin^2(\beta)}} - 1\right) \tag{17}$$

Now, with the aid of Eqs. (5) and (17), a relation for the hoop stress which is again function of the radial position can be obtained and thus formulations for all the principle stresses have been attained.

2.3. Incompressibility condition

Considering the small tubular ring shown in Fig. 4(b), expressions for the incompressibility condition in terms of the principal strains is given by

$$d\varepsilon_r + d\varepsilon_t + d\varepsilon_z = 0 \tag{18}$$

where the subscripts r, t, and z denote the radial, circumferential, and longitudinal directions.

2.4. Levy–Mises flow rule

It is worth noting that the principal strains represent an appropriate approximation of the principle plastic strains since the tube is subjected to a large plastic deformation. Therefore, from J2-plasticity, the equivalent plastic strain increment is defined by (Chakrabarty, 2006):

$$d\varepsilon_{ij} = S_{ij}d\lambda \tag{19}$$

$$\frac{d\varepsilon_r}{S_r} = \frac{d\varepsilon_t}{S_t} = \frac{d\varepsilon_z}{S_z} = d\lambda \tag{20}$$

where, $d\lambda = \frac{3}{2}\frac{d\varepsilon_e^p}{\sigma_e}$ and S_i are the deviatoric stress components and they are given by:

$$S_r = \frac{1}{3}(2\sigma_r - \sigma_z - \sigma_t) \tag{21}$$

$$S_t = \frac{1}{3}(2\sigma_t - \sigma_z - \sigma_r) \tag{22}$$

$$S_z = \frac{1}{3}(2\sigma_z - \sigma_t - \sigma_r) \tag{23}$$

Now, using Eqs. (20)–(23) we get:

$$d\varepsilon_r = \frac{(2\sigma_r - \sigma_z - \sigma_t)}{(2\sigma_t - \sigma_z - \sigma_r)}d\varepsilon_t \tag{24}$$

Combining Eqs. (24) and (5) yields:

$$d\varepsilon_r = \frac{(\sigma_r - \sigma_z - mY)}{(\sigma_r - \sigma_z + 2mY)}d\varepsilon_t \tag{25}$$

Mathematical manipulation of Eqs. (13) and (17) yields:

$$\sigma_r - \sigma_z = K_1\left(\left(\frac{r_{1o}}{r_{1i}}\right)^{K_3}\left(K_2 + \left(\frac{r}{r_{1i}}\right)^{-K_3}\right) - 1 - K_2\right) \tag{26}$$

where,

$$K_1 = \frac{mY}{1 - \sin^2(\beta)}$$

$$K_2 = \frac{\pi(r_{2i}^2 - r_{1i}^2)(1 + \mu\cot(\alpha))}{\pi(r_{1o}^2 - r_{1i}^2)}$$

$$K_3 = \frac{\left(\sin^2(\beta) - 1\right)}{\sin^2(\beta)}$$

Now, substitute from Eq. (26) into Eq. (25) yields:

$$d\varepsilon_r = \frac{K_1\left(\left(\frac{r_{1o}}{r_{1i}}\right)^{K_3}\left(K_2 + \left(\frac{r}{r_{1i}}\right)^{-K_3}\right) - 1 - K_2\right) - mY}{K_1\left(\left(\frac{r_{1o}}{r_{1i}}\right)^{K_3}\left(K_2 + \left(\frac{r}{r_{1i}}\right)^{-K_3}\right) - 1 - K_2\right) + 2mY}d\varepsilon_t \tag{27}$$

Again using Eqs. (20)–(23) we get:

$$d\varepsilon_z = \frac{(2\sigma_z - \sigma_t - \sigma_r)}{(2\sigma_t - \sigma_z - \sigma_r)}d\varepsilon_t \tag{28}$$

Combining Eqs. (28) and (5) yields:

$$d\varepsilon_z = \frac{-2(\sigma_r - \sigma_z) - mY}{(\sigma_r - \sigma_z) + 2mY}d\varepsilon_t \tag{29}$$

Substitute from Eq. (26) into Eq. (29) yields:

$$d\varepsilon_z = \frac{-2K_1\left(\left(\frac{r_{1o}}{r_{1i}}\right)^{K_3}\left(K_2+\left(\frac{r}{r_{1i}}\right)^{-K_3}\right)-1-K_2\right)-mY}{K_1\left(\left(\frac{r_{1o}}{r_{1i}}\right)^{K_3}\left(K_2+\left(\frac{r}{r_{1i}}\right)^{-K_3}\right)-1-K_2\right)+2mY}d\varepsilon_t \quad (30)$$

Now, considering that the principal strain increments given by Eqs. (27) and (30) can be expressed as $d\varepsilon_r = \frac{dt}{t}$, $d\varepsilon_t = \frac{dr}{r}$, $d\varepsilon_z = \frac{dz}{z}$, where dr, dt, and dz represents the incremental change in tubular's radius, thickness, and length at the expansion zone and the subscripts r, t, and z denote the radial, circumferential, and longitudinal directions, respectively. Then, Eqs. (27) and (30) can be solved numerically by integrating them over the following integration limits: $(t_1$–$t_2)$, $(r_{1i}$–$r_{2i})$, and $(z_1$–$z_2)$ in order to obtain the variations in the tubular thickness and length as a result of the change in the tubular radius. It is expected that the strains will be non-uniform over the wall thickness due to many reasons including material anisotropy, varying contact condition, non-uniform surface finish, etc. However, for the sake of simplicity, it has been assumed uniform strain over the wall thickness. Yet, by changing the integration limits from $(r_{1i}$–$r_{2i})$ to $(r_{1i}$–$r_{1o})$ one would be able to get an insight on the stress and strain variations over the wall thickness as given by Eq. (15).

2.5. Pressure limits of expanded pipe

Two important pressure limits, P_{Yi} and P_{Cr}, are considered to be of importance in the study of pressurized cylinders. P_{Yi} corresponds to the internal pressure that can be withstood by a pipe at the onset of yielding of the surface, while P_{Cr} is the external pressure required to cause the tubular wall to collapse. The nominal internal pressure rating of conventional casing pipes is calculated by using the historical API (American Petroleum Institute) equation or Barlow's equation. This equation is one-dimensional representation of the von Mises condition in association with a fairly accurate expression of the hoop stress in the pipe body. Current tendencies within the industry suggest that a more accurate calculation method of the designed yield pressure of conventional oil and gas tubulars is through the criterion proposed by von Mises which implies that the triaxial pipe body yield is influenced by a diverse number of stresses including bending stress, axial stress, and torsional stress. Based on this triaxial principle, a new formulation has been proposed for which the initial yield of the pipe body occurs when the stress applied in its working environment reaches the equivalent von Mises stress. Very recently, Sanchez and Al-Abri (2013) conducted a comparative study investigating the internal pressure rating of an open-end thick-wall pipe for the special case of purely internal pressure with the aid of Barlow and Triaxial formulations. It has been observed that the attained values using these two methods are very close with a difference in the vicinity of 1%. Thus, in the current study Barlow's Equation has been used again with the aim of studying the effect of expansion percentage and post-expansion outer-diameter-to-wall-thickness ratio (OD/t) on the internal pressure rating of the tubular at a fixed value of the yield strength that is equal to its original yield strength. However, there is no doubt that the yield strength after expansion would be different mainly due to the cold working process. But, due to the number of scenarios for which the yield strength needs to be attained, then the original value of the yield strength has been used in this study with the assumption that material remains isotropic after expansion. This study is one step ahead from the study conducted by Sanchez and Al-Abri (2013) in which an expression for the thickness variation which is one of two main factors that influence the internal pressure rating, namely the yield strength and the post-expansion geometry, has been attained. Thus, the upcoming work would be focused on addressing the variation in the post-expansion yield strength.

The collapse pressure of the tubular after expansion has been determined based on the petroleum and natural gas industries-equations for the properties of casing, tubing, drill pipe, and line pipe given in ISO/TR 10400 (2007). Based on the tubular grade and its outer-diameter-to-wall-thickness ratio, the formulations for calculating the collapse pressure have been classified into four regions. These are: yield strength collapse, plastic collapse, transition collapse, and elastic collapse. For example, by considering the L-80 Grade tubular which is similar to the one under consideration in this study, the OD/t value of the pre-expanded pipe corresponds to the range of plastic collapse (Table 6, ISO/TR 10400 (2007)). However, once the tubular is expanded both OD and t are notably modified to the point where, by assuming the same conventional material yield strength, the collapse behavior becomes transitional (Table 7, ISO/TR 10400 (2007)). Thus, in this study, all these cases have been programmed in MATLAB wherein, based on the post-expansion OD/t, the program picks the correct formulation and use it in the calculation.

3. Finite element analysis

The tubular expansion process was modeled using ABAQUS, a finite element analysis software. It is well known that a three-dimensional (3-D) FEA model is more realistic as compared to the simplified two-dimensional (2-D) axisymmetric model. However, due to the complexity and computational time considerations, a 2-D axisymmetric model shown in Fig. 5, was adopted for this work. But, at first, comparison between the 2-D and the 3-D models results has been done where the 2-D axisymmetric and the 3-D planar quarter symmetric models have been developed using 4-node quadrilateral (C2D4R) and 8-node linear brick (C3D8R) elements, respectively. Once converged, the 2-D axisymmetric representation was utilized as the standard simulation model in this work. A detailed comparison between the 2-D and the 3-D models was addressed and presented in (Pervez et al., 2008). The tubular and mandrel parameters are given in Table 1. The tubular was modeled as a deformable body with elastic–plastic material behavior; whereas the mandrel was modeled as a rigid body. The Mises yield surface was used to define the onset of plastic deformation. The hardening was assumed to be isotropic. A four-node bilinear axi-symmetric quadrilateral with reduced integration (CAX4R) element was used to model the tubular. The

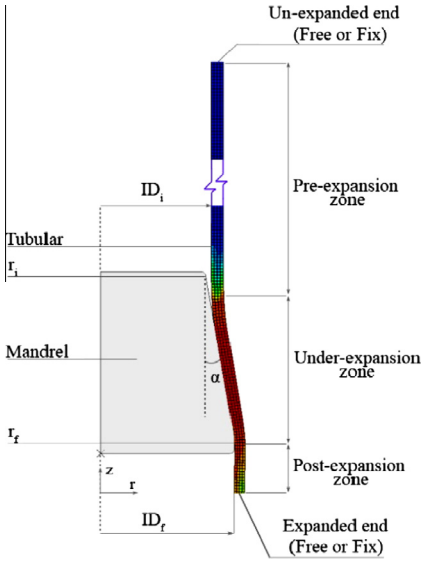

Fig. 5. 2D axi-symmetric finite element model of tubular–mandrel system.

Table 1
Finite element model input parameters.

Part	Parameters	Value
Tubular	Inner diameter (mm)	174.625
	Outer diameter (mm)	193.675
	Section length (mm)	3500.0
	Density (kg/m^3)	7800.0
	Young modulus (MPa)	82111
	Yield strength (MPa)	615.23
	Ultimate strength (MPa)	702.44
	Poisson ratio	0.3
	Failure strain	0.1966
	Coefficient of friction	0.06
	Stress–strain data	Fig. 6
Mandrel	Maximum outer diameter (mm)	209.55

induced friction between the tubular and mandrel was modeled using Coulomb friction law. The coefficient of friction was set at 0.06 so that it matches the actual test conditions. The mandrel cone angle was set at 10° to compare simulation results with experimental data. The edges of the cone were fillet of 3 mm radius to avoid stress concentration. Force required for expansion, contact pressure, and thickness and length variations were extracted from output database file of simulated cases. However, only results of force required to expand the tubular, reduction in tube wall thickness, and variation in tubular length are reported here and compared with available experimental data.

The tubular is made of high strength low-alloy steel with 0.23% carbon, 1.34% manganese, 0.23% silicon, 0.011% phosphorus and 0.002% sulphur. In oil and gas industry, these are referred as special LX80/LSX80 tubular. It has high yield and ultimate tensile strengths in the range of 600–620 MPa and 690–715 MPa, respectively. The material properties of the tubular were obtained based on uni-axial tensile tests conducted on specimens following ASTM standard test methods. Three samples were tested in tension on Universal Testing Machine till it fractured. ASTM E8 has been used to define the test procedure. Determination of the Young's modulus has been done in accordance with ASTM E111. Yield strength, ultimate tensile strength, elongation, and strain at fracture have been extracted from the attained stress–strain curve. The stress–strain curves for three samples are shown in Fig. 6. Average properties based on these tests were used in finite element analysis. The hardening curve data required in ABAQUS software was provided in the tabular form where the first pair of numbers corresponds to the initial yield stress at zero plastic strain. To simulate the down-hole expansion process, the lower end of the tubular was held fixed while the upper end was kept free. This resembles jack and anchor approach used in well drilling.

4. Experimental study

Experimental tests of tubular expansion processes were conducted to validate the developed analytical and numerical models.

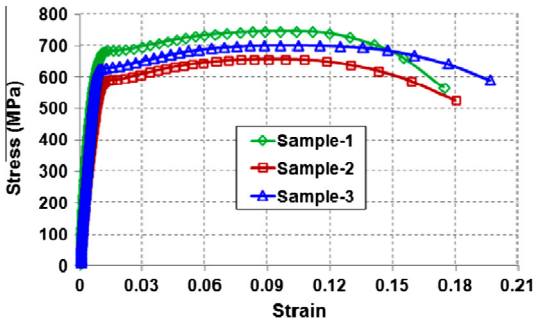

Fig. 6. Stress–strain curve for the as-received tubular material.

They were carried out in the recently designed and commissioned expandable tubular test-rig in the Engineering Research Laboratory at Sultan Qaboos University (see Fig. 7). In terms of capacity, the test-rig is capable of expanding tubular sizes ranging from 2–7/8 in (73.025 mm) to 9–5/8 in (244.475 mm) with expansion percentages varying from 10% to 30%. Furthermore, the test-rig is capable of testing tubular under fixed-free and fixed–fixed end conditions for pipes of lengths varying from 2 to 10 m. Also, it is provided with hydraulic pumps that are capable of supplying 2350 bar at 11 l/min or 700 bar at 50 l/min. To resemble the cone-on-stick approach that is usually adopted in the oil and gas industry, the test-rig is provided with a hydraulic cylinder that is capable of delivering mechanical pull force up to 140 metric-tons.

The current tests were performed on specimens of standard expandable tubulars for oil well applications of 193.68 mm outer diameter and 9.53 mm wall thickness. The tubular specimens were expanded using mandrels of [203.2, 209.55, and 215.9] mm outer diameters representing three expansion ratios of 16.4%, 20.0% and 23.7% of the tubular inner diameter. Fig. 8 summarizes the procedure adopted to prepare the tubular specimens for the experimental expansion tests. First, the mandrel was entered into a small tubular segment by means of a mechanical pressing machine (Fig. 8(a)). This part is known as launcher. The launcher was then welded from one side into a longer tubular segment (Fig. 8(b)) that needs to be expanded while the other side was welded to a flange (Fig. 8(c)) producing a small chamber behind the mandrel that was used to accumulate the hydraulic pressure in order to push the mandrel forward. In down-hole applications, the tubular is usually deployed to a specific depth with the mandrel attached to it. Then, it is anchored in place by fixing one of its ends (i.e., front or rear end as shown schematically in Fig. 9). The anchoring is usually done against the formation in open-hole applications or against another tubular in cased-hole applications, and then the expansion process is executed. Thus, the flange has another purpose which is to anchor the tubular from one of its end resembling the actual situation. In order to grantee the alignment of the mandrel during the expansion process, an aligner made of two discs separated by a distance with diameters equal to the drift diameter of the tubular were used. Then, the tubular-mandrel system was mounted on the test-rig (Fig. 8(d)). After that, the high pressure line was connected to the flange in order to supply the system with the hydraulic fluid required to push the mandrel forward (Fig. 8(e)). A view of the experimental setup just before the start of the test is shown in Fig. 8(f).

In order to obtain measurable quantities for analysis, the test-rig is provided with instrumentation and control system to monitor, control and store data for many system variables. These

Fig. 7. Expandable Test Rig (ETR) at Engineering Research Lab (ERL), SQU.

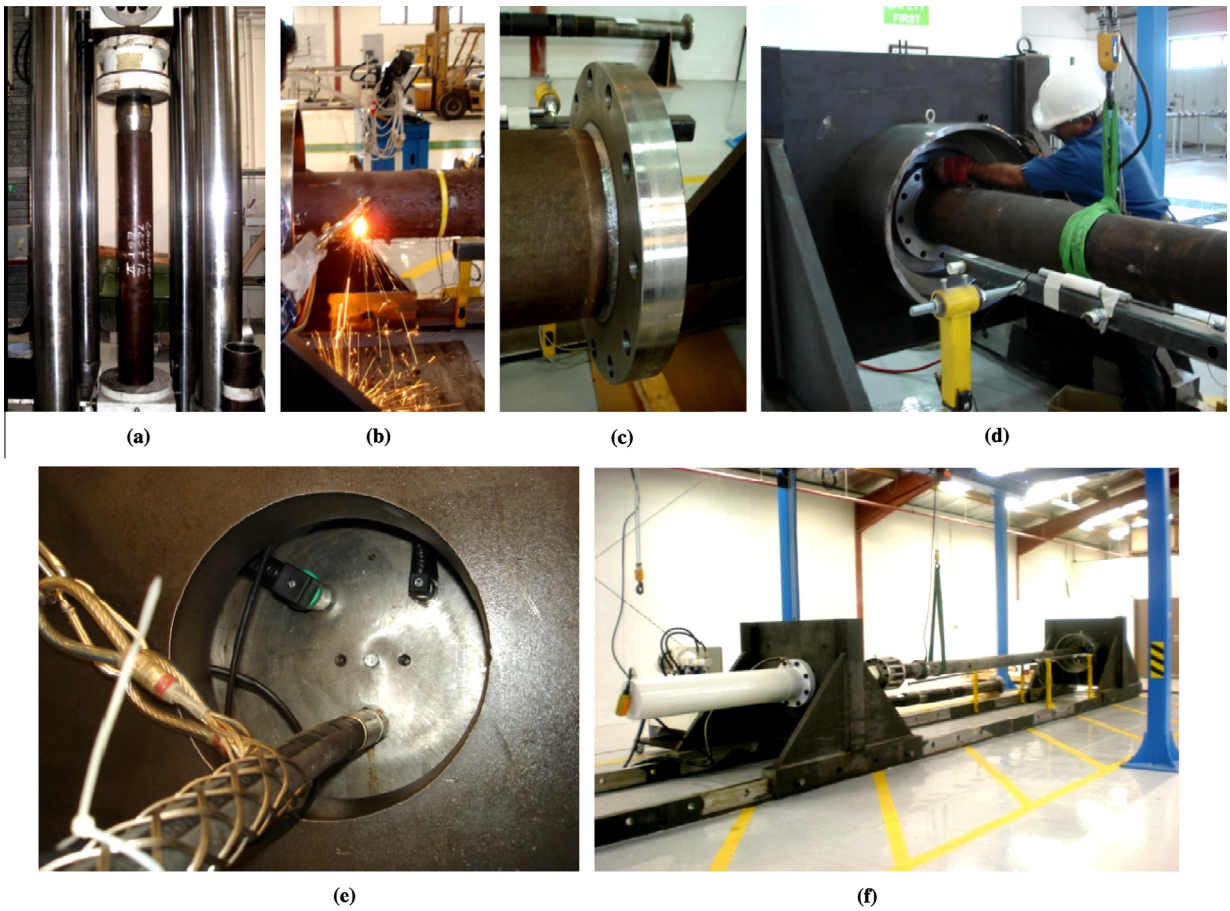

Fig. 8. Experimental test setup procedure: (a) create launcher using mechanical pressing machine; (b) welding launcher to longer pipe section; (c) flange welded to the launcher; (d) mounting tubular–mandrel system in the test-rig; (e) high pressure line connected to the flange; (f) pipe ready for test.

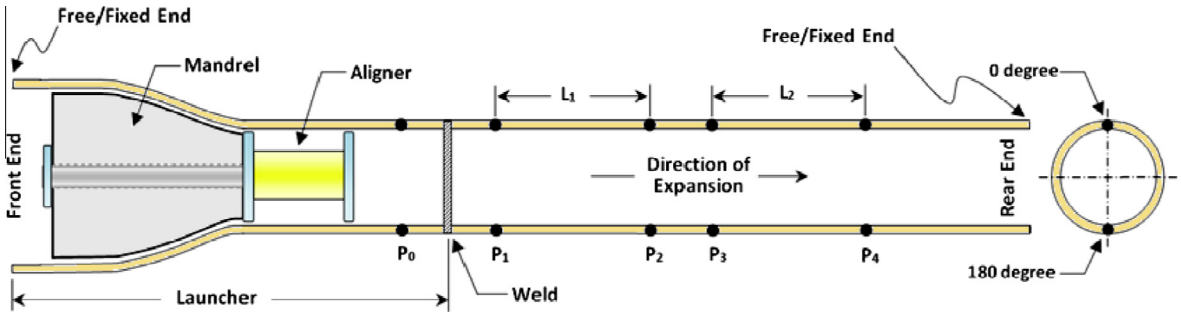

Fig. 9. Schematic diagram of the expandable tubular test setup.

variables include strain, diametrical displacement, expansion force, tubular thickness and length variations, operating fluid temperature, flow rate, and speed and location of expansion mandrel. In the current setup, three pressure sensors one at the outlet of the hydraulic unit and the other two at the flange were used to measure the hydraulic pressure supplied to the mandrel–tubular system online. Also, an ultrasonic distance sensor was used and mounted at the rear end to monitor the mandrel position as it moves along the tubular during the expansion process. The variation in outside diameter is precisely measured through LVDT's (Linear Voltage Displacement Transducer); mounted on each side of the tubular (0° and 180°). Pre- and post-expansion thickness measurements were taken using a TI-25DL ultrasonic wall thickness gauge at five different locations (P_i, $i = 0,1,2,3,4$) on the outer surface of the tubular. At every location, two points (0° and 180°) are selected along the circumferential direction, as shown in Fig. 9. The method that was used to find out the change in the tubular length was to draw straight lines of known length (L_1 and L_2) along the outer surface of the tubular before the expansion process, and then to measure them again after the expansion was completed, thus giving the amount of length variation caused by the expansion process. Pre- and post-expansion material properties of the tube are determined following ASTM standard test methods including hardness, Young's Modulus, yield and ultimate tensile strengths, ductility, and strain at fracture.

5. Results and discussions

It is necessary for field engineers to estimate the expansion requirements before proceeding with any expansion work in order to select appropriate expansion tools and avoid any unexpected failure. A prior knowledge of required expansion force and expansion procedures for a specific expansion ratio and tubular size is extremely important. Several factors do affect the solid tubular expansion process; however this work is focusing on parameters which are important for well engineering applications. These are expansion force (F_e), expansion ratio (ER), friction coefficient (μ), mandrel angle (α), collapse pressure rating (P_{Cr}), and the maximum operating pressure that can be sustained by the tubular before it starts to yield (P_{Yi}). Experimental, numerical and/or analytical techniques have been adopted in this work to find out the effect of these parameters. However, since the actual testing procedure is cumbersome and usually requires careful selection of tools and its execution, only few cases have been tested experimentally based on which analytical and/or finite element solutions have been developed, validated and employed for further investigation. In this work, expansion ratios ranging from 0% to 40% are considered. The friction coefficient is varied between 0 and 0.35 with an increment of 0.05. Also, the mandrel angle is varied between 5° and 50° with a step of 5°.

A 3.5 m long tubular having geometrical and material parameters as given in Table 1 was used for both experimental and simulation studies. In experimental part of work, three tubular specimens were expanded to three different percentages of 16.4%, 20.0% and 23.7% of the tubular inner diameter. This is attained using three mandrels of [203.2, 209.55, and 215.9] mm outer diameters. At first, the finite element analysis results have been verified using experimental data. Later, the finite element model was used to validate the developed analytical model. Finally, using the analytical model, a parametric study of the effect of expansion percentage, mandrel angle, contact conditions at mandrel/tubular interface, and the tubular size, on the expansion force, thickness and length variations, collapse pressure rating, and maximum operating pressure before the tubular starts yield have been accomplished.

5.1. Finite element model validation

Figs. 10–12 show a comparison between experimental and finite element model results at fixed expansion ratio of 20%, fixed mandrel angle of 10°, and fixed friction coefficient of 0.06. Fig. 10 shows the expansion force required to push the mandrel forward inside the tubular. It is found that the expansion force required for 20% expansion ratio obtained through simulation is in good agreement with the experimental results with an error of less than 4%. In all cases, the expansion force initially reached a peak value

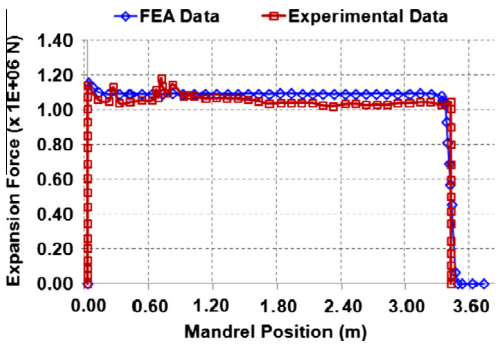

Fig. 10. Variation in expansion force along tubular length for 20% expansion ratio.

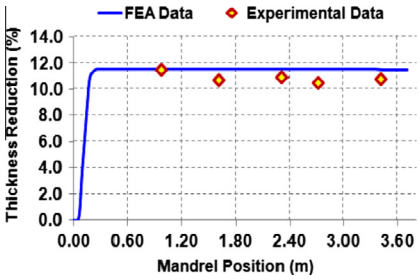

Fig. 11. Thickness reductions for 20% expansion ratio.

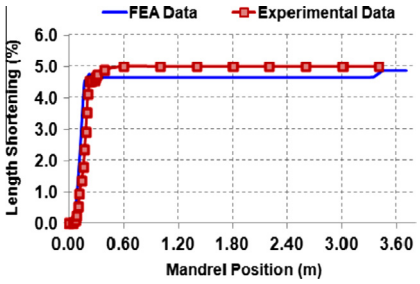

Fig. 12. Length shortening for 20% expansion ratio.

and then drops down to an almost steady-state value. The initial peak force was 1160 kN and then stabilized to an average value of 1080 kN during the rest of the expansion process. Small fluctuations in the expansion force were observed during transient period but overall the process is stable. The maximum value of force attained at the beginning of the expansion process represents the initial upsetting behavior caused by the material resistance to change in its form. In the tube expansion process, the flow of the tubular material is caused by the pressure transmitted from the mandrel to the deforming tubular. The frictional conditions at the mandrel/tubular interface greatly influence the metal flow, formation of surfaces, stresses acting on the mandrel, and the load and energy requirements. One would think that by using the simple Coulomb friction law the frictional effects would be constant along the interface. This is true but not during the transient regions. By recalling that the Coulomb friction also depends on the normal forces which may vary during the transient regions of the process, then the presence of an initial peak at the beginning of the process can be justified by recalling the typically high stress value is may be due to the natural resistance of the material to any change in its form. Such resistance vanishes as the material starts to flow making the process to be smoother

Figs. 11 and 12 show the variations in tubular thickness and length for 20% expansion ratio, respectively. Tubular thickness, before and after expansion, were measured at ten different locations, and an average value of thickness reduction was calculated for comparison with simulation results. Similarly, the length shortening was measured at the beginning and the end of the tubular. Again, the average value was calculated for comparison with simulation results. There is an excellent agreement in case of length shortening, while for thickness reduction the difference is in the vicinity of 10%.

5.2. Analytical model validation

Now, using the validated finite element model along with the three set of experimental data, a comparison between experimental, analytical and finite element results of expansion force, thickness reduction and length shortening were performed as

presented in Figs. 13–15. It is clear from the comparison that the finite element results are in good agreement with the experimental results, and the developed analytical model is capable of mimicking them with minor discrepancies. Fig. 13 is showing the expansion force as function of the friction coefficient and mandrel angle for various expansion ratios. It is obvious from the figure that at fixed friction coefficient and mandrel angle, the expansion force increases linearly with the expansion ratio.

A prior understanding of the geometrical characteristics of the tubular in the post-expansion phase, such as length and thickness variations, is of critical importance for careful selection of tools and its execution in the course of designing a well. These will allow the designers to use the appropriate tools, avoid length gaps in the overlap regions between two consecutive tubular patches, and correctly determine the post-expansion collapse and burst strengths of the tubular due to thickness variations. The thickness and length variations for various expansion ratios are shown in Figs. 14 and 15. It is obvious from the figures that the tubular thickness and length decreases as the expansion ratio increases, resulting in tube thinning and shortening. The wall thickness of the tubular is linearly decreased when expansion ratio increases. The maximum discrepancy in the analytical model results was found in the estimation of the length shortening of the tubular which is one of the key factors for the successful field applications of this technology. From an operational point of view, positioning the tubular at the planned target depth is very difficult, and consequently may be positioned somewhat higher/lower than where it suppose to be. Such wrong positing of the tubular without adequate information about the amount of tubular shortening due to the expansion process would affect the anchoring of the tubular to the previous casing strings as well as it may cause inadequate coverage of troublesome zones. However, this issue can be alleviated easily as the amount of discrepancy is only few percentages and is possible to take care of through the safety factors.

It is worth noting that an increase in the expansion ratio results in an increase in the expansion force and a decrease in the tubular thickness and length resulting in tubular thinning and shortening. The relationship is almost linear in all the cases. It is obvious from Fig. 13 that expanding the tubular to 28% of its original inner diameter needs a force of more than three times the one required for the 12% expansion ratio. Also, going from 12% ER to 28% ER causes 8% additional thickness reduction and 3.5% extra length shortening in the tubular as depicted in Figs. 14 and 15, respectively.

5.3. Parametric study

A parametric study to determine the effect of four main factors, including: expansion percentage, mandrel configuration, friction coefficient, and tubular size, on the expansion force, length and thickness variations, collapse pressure rating, and the maximum operating pressure, has been done using the developed analytical model. A 3D surface fitting of the results obtained from the analytical model has been done using MATLAB software. Fig. 16 shows the effect of changing mandrel configuration (mandrel angle) on the force required for achieving certain expansion ratio. It is clear from the figure that for a fixed coefficient of friction, the expansion

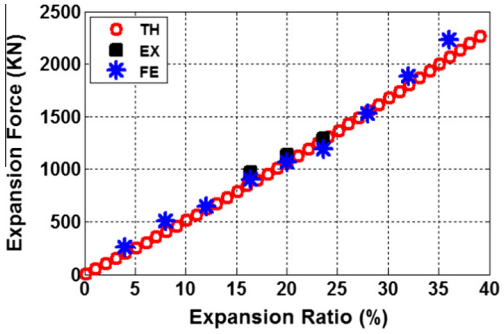

Fig. 13. Analytical (TH), experimental (EX) and finite element (FE) results of expansion force at different expansion ratios with $\alpha = 10^\circ$ and $\mu = 0.06$.

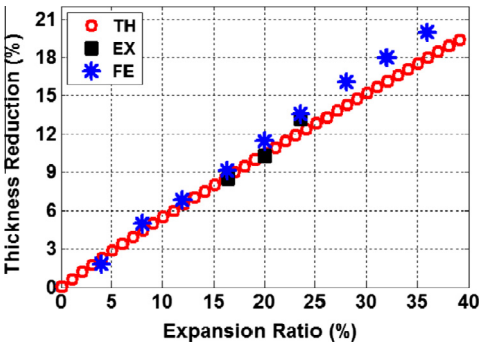

Fig. 14. Analytical (TH), experimental (EX) and finite element (FE) results of thickness reduction at different expansion ratios with $\alpha = 10^\circ$ and $\mu = 0.06$.

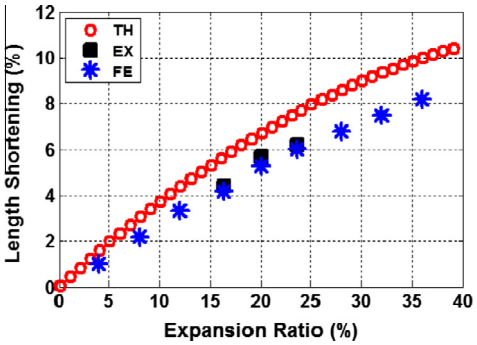

Fig. 15. Analytical (TH), experimental (EX) and finite element (FE) results of length shortening at different expansion ratios with $\alpha = 10^\circ$ and $\mu = 0.06$.

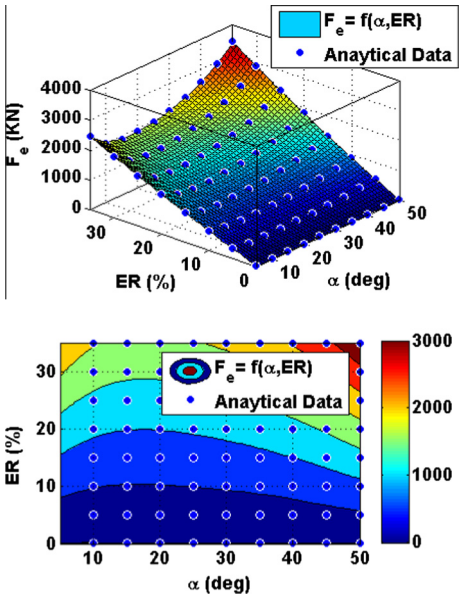

Fig. 16. Expansion force (F_e) for different mandrel cone angles (α) and different expansion ratios (ER) at fixed friction coefficient (μ) of 0.06.

force decreases as the mandrel angle increases. The minimum value does not occur at one value of the angle rather it varies between 15° to 20° depending on the expansion percentage. Such reduction in the force with the increase in mandrel angle can be attributed to the reduction in contact area between mandrel and the tubular resulting in lower shear effects between the two surfaces. Fig. 17 is showing the effect of changing mandrel angle on tubular thickness at different values of the expansion ratio. It is clear from the figure that the reduction in tubular thickness exhibits small change as the mandrel angle increases at a fixed expansion ratio with a minimum thickness reduction occurs in the vicinity of the 20° angle and then it increases as we go above or lower than this value. On the other hand, Fig. 18 is showing the opposite behavior for tubular length. This can be justified by considering the reduction in contact area between mandrel and the

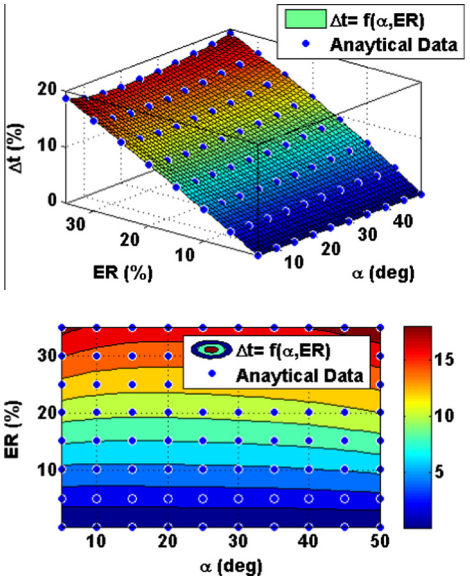

Fig. 17. Thickness reduction (Δt) for different mandrel cone angles (α) and different expansion ratios (ER) at fixed friction coefficient (μ) of 0.06.

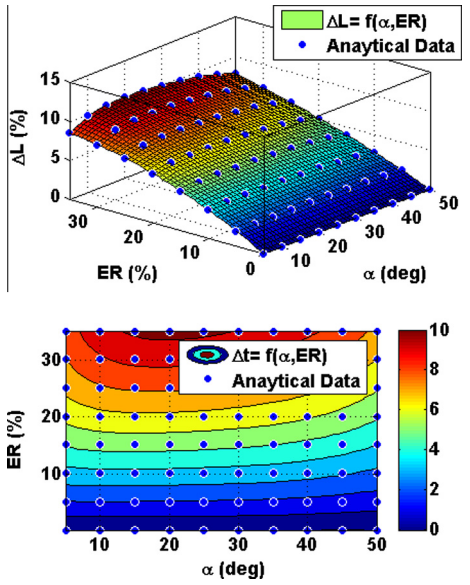

Fig. 18. Length shortening (ΔL) for different mandrel cone angles (α) and different expansion ratios (ER) at fixed friction coefficient (μ) of 0.06.

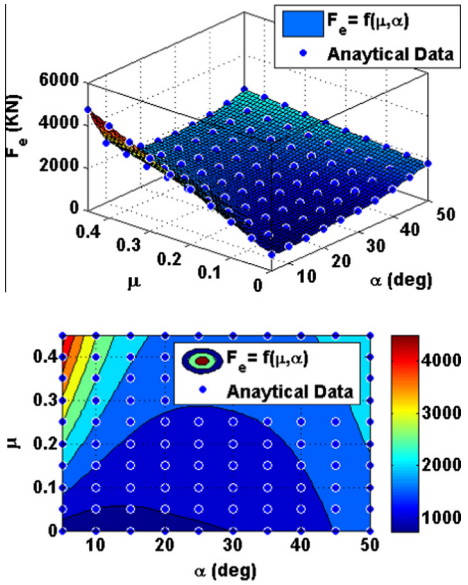

Fig. 19. Expansion force (F_e) for different mandrel cone angles (α) and different friction coefficients (μ) at fixed expansion ratios (ER) of 20%.

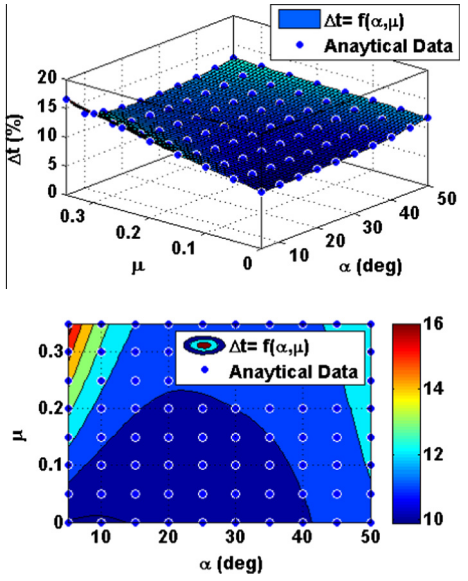

Fig. 20. Thickness reduction (Δt) for different mandrel cone angles (α) and different friction coefficients (μ) at fixed expansion ratios (ER) of 20%.

tubular by increasing mandrel angle. Therefore, large mandrel angle means small contact area, which results in less thickness reduction and more length shortening. Similarly, Figs. 19–21 are showing a parametric study for the effect of changing the coefficient of friction and mandrel angle at fixed expansion ratio on the expansion force and the structural integrity of the tubular. It is evident from Fig. 19 that for a fixed mandrel angle, the expansion force increases with the increase of friction coefficient. In Fig. 20, the effects of changing the friction coefficient on the tubular thickness are presented. It is clear from the graph that the magnitude of thickness reduction increases with the coefficient of friction for a constant mandrel angle. However, this variation is very small in the vicinity of the optimum mandrel angle of 20°. On the other hand, variation in tubular length in case of variable friction coefficient and constant mandrel angle is showing the opposite

behavior. This behavior is shown in Fig. 21. Length shortening phenomenon is observed to be more for small friction coefficient but the variation in length tends to become positive (i.e., elongate) for higher friction coefficients (i.e., greater than 0.4) and small mandrel angles (i.e., less than 10°). In most of the cases, the tubular length shortens for small values of friction coefficient as well as moderate mandrel angles. However, the higher expansion forces at the higher friction coefficient are causing the expanded section to elongate due to the tubular extension. This can be attributed to the resistance that opposes the interface materials from flowing smoothly over each other creating some tension in the tubular. But since this is only at higher value of friction coefficient along with small mandrel angle which may rarely be encountered in the real applications, then Fig. 21 has been designed to fit the real application ranges. However, the elongation observation can be easily established by considering Eq. (30) with the above mentioned values. Therefore, it can be concluded that the variation in tubular length mainly depends on the magnitude of expansion force which in turn depends on expansion ratio, drag, and mandrel angle.

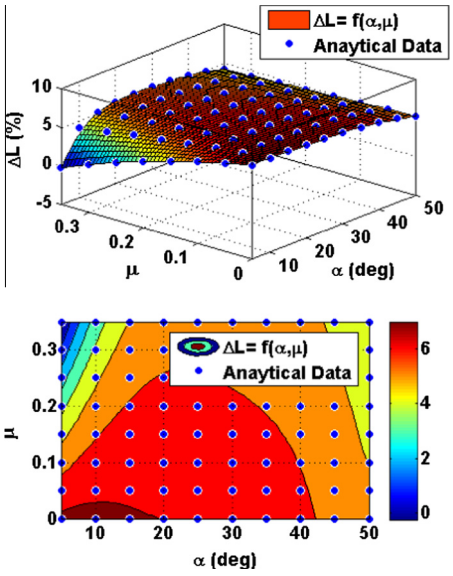

Fig. 21. Length shortening (ΔL) for different mandrel cone angles (α) and different friction coefficients (μ) at fixed expansion ratios (ER) of 20%.

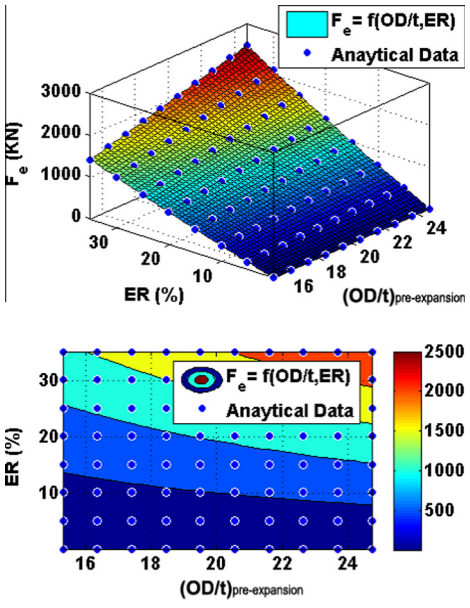

Fig. 22. Expansion force (F_e) for different pre-expansion outer-diameter-to-wall-thickness ratio (OD/t) and different expansion ratios (ER) at fixed wall thickness and mandrel configuration.

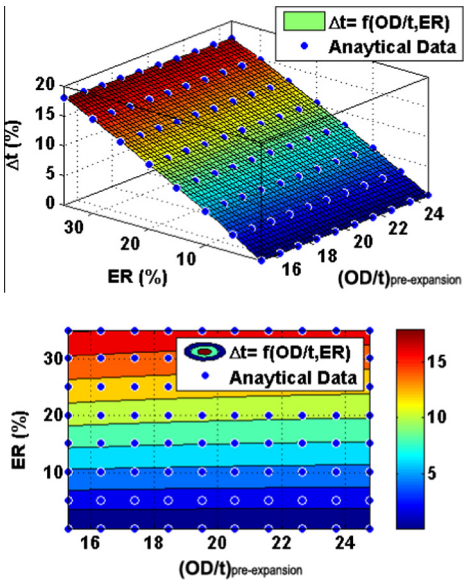

Fig. 23. Thickness reduction (Δt) for different pre-expansion outer-diameter-to-wall-thickness ratio (OD/t) and different expansion ratios (ER) at fixed wall thickness and mandrel configuration.

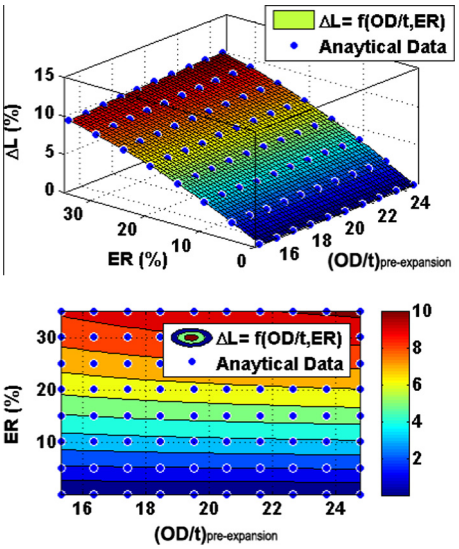

Fig. 24. Length shortening (ΔL) for different pre-expansion outer-diameter-to-wall-thickness ratio (OD/t) and different expansion ratios (ER) at fixed wall thickness and mandrel configuration.

Now, let's consider the change in tubular geometry and it effect on the expansion force, length, and thickness variations of the tubular. Fig. 22 shows the value of the force required to expand tubular with different pre-expansion outer-diameter-to-wall-thickness ratios. It is important to highlight that the variation in the tubular cross-section has been done by changing the inner-diameter and the outer-diameter of the tubular while keeping the thickness as constant. It is interesting to observe that tubulars with small outer-diameter-to-wall-thickness ratios (i.e., small cross-section) require much less force as compared to the ones of

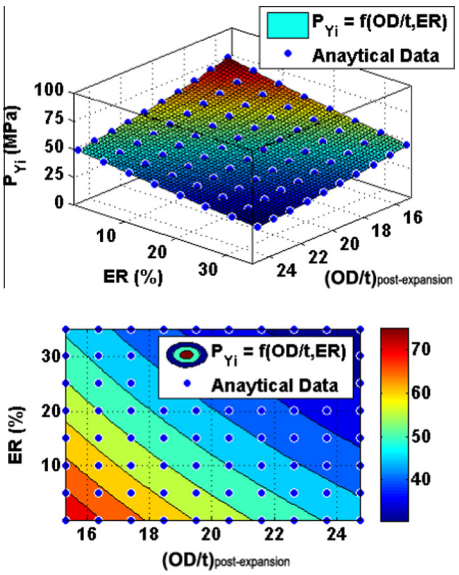

Fig. 25. Maximum operating pressure at the onset of yielding (P_{Yi}) for different post-expansion outer-diameter-to-wall-thickness ratio (OD/t) and different expansion ratios (ER) at fixed wall thickness and mandrel configuration.

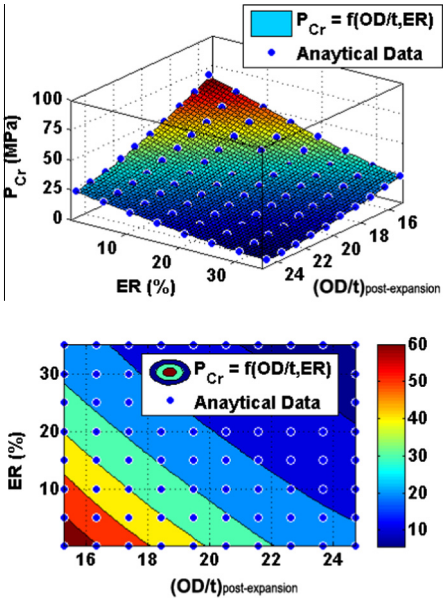

Fig. 26. Predicted collapse pressure (P_{Cr}) for different post-expansion outer-diameter-to-wall-thickness ratio (OD/t) and different expansion ratios (ER) at fixed wall thickness and mandrel configuration.

bigger outer-diameter-to-wall-thickness ratio especially for higher expansion ratios. However, the effects of the cross-section on the structural variation of the tubular are almost negligible with the change in expansion ratio as clearly shown in Figs. 23 and 24. This means that tubulars with small cross-section needs a small expansion force as compared to the bigger cross-section tubes when they are subjected to high expansion ratios, while there is almost no effect on the geometrical variations of the tubular.

An investigation on the effect of the expansion process on the pressure limits of an expanded pipe due to the effect of an internal pressure is depicted in Fig. 25. The investigation studied the effect of the expansion ratio and the post-expansion outer-diameter-to-wall-thickness (OD/t) ratio on the maximum operating pressure that a tubular can withstand before it starts to yield at a fixed value of the yield strength that is equal to its original yield strength. However, there is no doubt that the yield strength after expansion would be different mainly due to the cold working process. But, due to the number of scenarios for which the yield strength needs to be attained, then the original value of the yield strength has been used in this study such that the focus will be on the effect of the geometrical variations. It is evident from the figure that the amount of internal pressure that can be withstand by a tubular of small post-expansion outer-diameter-to-wall-thickness (OD/t) ratio is higher than that of big OD/t. These values are decreasing as the expansion ratio increases due to the reduction in the tubular wall thickness. The same observations can be generalized for the collapse pressure rating depicted in Fig. 26. However, it is important to emphasize that the value of the maximum operating pressure before the tubular starts to yield is higher than that of the collapse pressure rating. Thus, the likelihood of the tubular to get damaged from an externally applied pressure is higher than that may occur because of the internal applied pressure.

6. Conclusions

Analytical and numerical models describing the expansion process of a thick-wall solid tubular have been developed based on kinematics and equilibrium conditions. In addition, tubular expansion tests have been conducted in the expandable tubular test-rig at SQU, to validate the developed analytical and numerical models. It was found that the results for expansion force, thickness reduction and length shortening under various expansion ratios from both models are in good agreement with the experimental observations. It is also evident from the comparison that the expansion of the tubular by 16%, 20%, and 24% expansion ratios result in thickness reduction of approximately 6.67%, 10.3%, and 13.16%, and length shortening of approximately 4.4%, 5.7%, and 6.2%, respectively. Also, the expansion force increases as the expansion ratio and the friction coefficient increases while it decreases as the mandrel angle increases due to the reduction in contact area. Tubular wall thickness decreases as the expansion ratio and the friction coefficient increases while the reduction in wall thickness reduces as the mandrel angle increases. Also, it has been observed that the tubular length shortens for most of the loading mechanisms. However, it elongates sometimes at higher values of friction coefficient (i.e., greater than 0.4) and small mandrel angles (i.e., less than 10°). This can be attributed to the difficulty that opposes the interface materials from flowing over each other smoothly creating some tension in the tubular. Finally, it is worthwhile to state that the developed analytical and numerical models are capable of providing excellent approximation for the actual experimental results, which consequently would help in reducing the trial and error operations in the selection of tools and processes design and thereby reduce material waste and lead-time to drill new wells.

Acknowledgments

The authors would like to thank Sultan Qaboos University (SQU) and Petroleum Development Oman (PDO) for their financial support, which would not have been possible to conduct this work without it. Useful discussion with members of the Applied Mechanics and Advanced Materials Research Group (AM^{2}RG) is highly appreciated. All the experimental work was done with the assistance of Dr. Siegfried Trautwein and Mr. Ahmed S. Faiz.

References

Al-Dhafeeri, A.M., Nasr-El-Din, H.A., 2007. Characteristics of high-permeability zones using core analysis and production logging data. Journal of Petroleum Science and Engineering 55 (1–2), 18–36.

Al-Hiddabi, S.A., Seibi, A.C., Pervez, T., 2002. Stress analysis of casings expansion/post-expansion: theoretical approach. In: ASME 6th Biennial Conference Engineering Systems Design and Analysis (ESDA2002/APM-92), Istanbul, Turkey.

Ayob, A.B., Tamin, M.N., Elbasher, M.K., 2009. Pressure limits of thick-walled cylinders. In: Proceedings of the International MultiConference of Engineers and Computer Scientists (IMECS 2009), Vol. II, Hong Kong.

Benzie, S., Burge, P., Dobson, A., 2000. Towards a mono-diameter well – advances in expanding tubing technology. In: SPE European Petroleum Conference, Paris, France, SPE paper # 65184.

Campo, D., Williams, C., Filippov, A., Cook, L., Brisco, D., Dean, B., Ring, L., 2003. Monodiameter drilling liner – from concept to reality. In: SPE/IADC Drilling Conference, Amsterdam, Netherlands, SPE/IADC paper # 79790.

Chakrabarty, J., 2006. Theory of Plasticity, third ed. Elsevier Butterworth, Heinemann, UK.

Chilingraian, G.V., Mazzullo, S.J., Rieke, H.H., 1996. Carbonate reservoir Characterization: A Geologic-Engineering Analysis. Elsevier, Amsterdam, Part II.

Darijani, H., Kargarnovin, M.H., Naghdabadi, R., 2009. Design of thick-walled cylindrical vessels under internal pressure based on elasto-plastic approach. Materials and Design 30 (9), 3537–3544.

Dupal, K.K., Campo, D.B., Lofton, J.E., Weisinger, D., Cook, R.L., Bullock, M.D., Grant, T.P., York, P.L., 2001. Solid expandable tubular technology – a year of case histories in the drilling environment. In: SPE/IADC Drilling Conference, Amsterdam, Netherland, SPE/IADC paper # 67770.

Escobar, C., Dean, B., Race, B., Waddell, K., 2003. Increasing solid expandable tubular technology reliability in a myriad of downhole environment. In: SPE Latin American and Caribbean Petroleum Engineering Conference, Port-of-Spain, Trinidad and Tobago, SPE paper # 81094.

Filippov, A., Mack, R., Cook, L., Yourk, P., Ring, L., McCoy, T., 1999. Expandable tubular solutions. In: SPE Annual Technical Conference and Exhibition, Houston, Texas, SPE paper # 56500.

Fokker, P.A., Verga, F., Egberts, P.J.P., 2005. New semianalytic technique to determine horizontal well productivity index in fractured reservoirs. SPE Reservoir Evaluation and Engineering 8 (2), 123–131.

Gao, X.-L., 2003. Elasto-plastic analysis of an internally pressurized thick-walled cylinder using a strain gradient plasticity theory. International Journal of Solids and Structures 40, 6445–6455.

Gusevik, R., Merritt, R., 2002. Reaching deep reservoir targets using solid expandable tubulars. In: SPE Annual Conference and Exhibition, San Antonio, Texas, SPE paper # 77612.

Hausenbauer, G.F., Lee, G.C., 1966. Stress in thick walled conical shells. Nuclear Engineering and Design 3 (3), 394–401.

ISO/TR 10400, 2007. Petroelum and natural gas industries – equations and calculations for the properties of casing, tubing, drill pipe and line pipe used as casing or tubing, firs ed., International Organization for Standardization (ISO), 2007, pp. 12–13.

Karrech, A., Seibi, A.C., 2010. Analytical model for the expansion of tubes under tension. Journal of Materials Processing Technology 210 (2), 356–362.

Klever, F.J., Stewart, G., 1998. Analytical burst strength prediction of OCTG with and without defects. In: SPE Applied Technology Workshop on Risk Based Design of Well Casing and Tubing, The Woodlands, Texas, SPE paper # 48329.

Lighthelm, D.J., van den Hoek, P.J., Hos, P., Faber, M.J., Roeterdink, R.C., 2006. Improved oil recovery in fractured carbonate reservoirs: do not give induced fractures a chance. In: SPE Europec/EAGE Annual Conference and Exhibition, Vienna, Austria, SPE paper # 98386.

Mack, R.D., McCoy, T., Ring, L., 1999. How in situ expansion affects casing and tubing properties. World Oil 220 (7), 69–70.

Mack, R.D., Filippov, A., Kendziora, L., Ring, L., 2000. In situ expansion of casing and tubing – effect on mechanical properties and resistance to sulfide stress cracking. In: NACE International, Orlando, Florida, Paper # 00164.

Marketz, F., Leuranguer, C., Welling, R.W.F., Ogoke, V., 2005. Waterflood appraisal-well delivery with expandable tubular. In: International Petroleum Technology Conference, Doha, Qatar, Paper # IPTC-10345.

Owoeye, O.O., Aihevba, L.O., Hartmann, R.A., Ogoke, V.C., 2000. Optimization of well economics by application of expandable tubular technology. In: SPE/IADC Drilling Conference, New Orleans, Louisiana, SPE/IADC paper # 59142.

Ozkaya, S.I., Richard, P.D., 2006. Fractured reservoir characterization using dynamic data in a carbonate field, Oman. SPE Reservoir Evaluation and Engineering 9 (3), 227–238.

Perry, J., Aboudi, J., 2003. Elastic–plastic stresses in thick-wall cylinders. ASME Journal of Pressure Vessel Technology 125, 248–252.

Pervez, T., 2010. Experimental and numerical investigations of expandable tubular structural integrity for well applications. Journal of Achievements in Materials and Manufacturing Engineering 41 (1–2), 147–154.

Pervez, T., Qamar, S.Z., 2011. Finite element analysis of tubular ovality in oil well. Advanced Materials Research 264–265, 1654–1659.

Pervez, T., Seibi, A.C., Karrech, A., 2005. Simulation of solid tubular expansion in well drilling using finite element method. Journal of Petroleum Science and Technology 23 (7–8), 775–794.

Pervez, T., Qamar, S.Z., Seibi, A.C., Al-Jahwari, F.K., 2008. Use of SET in cased and open holes: comparison between aluminum and steel. Journal of Materials and Design 29 (4), 811–817.

Pervez, T., Qamar, S.Z., Al-Hiddabi, S.A., Al-Jahwari, F.K., Marketz, F., Al-Houqani, S., vd Velden, M., 2011. Tubular expansion in irregularly shaped boreholes – computer simulation and field measurement. Journal of Petroleum Science and Technology 29 (7), 735–744.

Pervez, T., Al-Abri, O.S., Qamar, S.Z., Al-Busaidi, A.M., 2012a. Optimum mandrel configuration for efficient down-hole tube expansion. In: Proceedings of the ASME 11th Biennial Conference on Engineering Systems Design and Analysis (ESDA2012), Nantes, France, ESDA2012 paper # 82397.

Pervez, T., Qamar, S.Z., Al-Abri, O.S., Khan, R., 2012b. Experimental and numerical simulation of in situ tube expansion for deep gas wells. Materials and Manufacturing Processes 27 (7), 727–732.

Ruan, C.G., Maurer, W.C., 2005. Analytical model for casing expansion. In: SPE/IADC Drilling Conference, Amsterdam, Netherlands, SPE/IADC paper # 92281.

Ruggier, M., Benzie, S., Urselmann, R., Mosser, H., van Noort, R., 2001. Advances in expandable tubing – a case history. In: SPE/IADC Drilling Technology Conference, Amsterdam, Netherlands, SPE/IADC paper # 67768.

Sanchez, F.J., Al-Abri, O.S., 2013. Tube expansion under various down-hole end conditions. The Journal of Engineering Research 10 (1), 25–40.

Seibi, A.C., Al-Hiddabi, S.A., Pervez, T., 2005. Structural behavior of solid tubular expansion under large plastic deformation. ASME Journal of Energy Resources and Technology 127 (4), 323–326.

Seibi, A.C., Pervez, T., Al-Hiddabi, S.A., Karrech, A., 2006. Coupled stress and pressure waves propagation in an elastic solid tube submerged in fluids. Journal of Energy Resources Technology 128 (4), 247–256.

Seibi, A.C., Karrech, A., Pervez, T., 2007. Post-expansion tube response under mechanical and hydraulic expansion – a comparative study. Journal of Pressure Vessels Technology 129 (1), 118–124.

Seibi, A.C., Karrech, A., Pervez, T., Al-Hiddabi, S.A., Al-Yhamadi, A., Al-Shabibi, A., 2009. Dynamic effects of mandrel/tubular interaction on downhole solid tubular expansion in well engineering. Journal of Energy Resources Technology 131 (1), 013101–013108.

Stewart, G., Klever, F.J., 1998. Accounting for flaws in the burst strength of OCTG. In: SPE Applied Technology Workshop on Risk Based Design of Well Casing and Tubing, The Woodlands, Texas, SPE paper # 48330.

Stewart, R.B., Marketz, F., Lohbeck, W.C.M., Fischer, F.D., Daves, W., Rammerstorfer, F.G., Bohm, H.J., 1999. Expandable wellbore tubulars. In: SPE Technical Symposium, Dhahran, Saudi Arabia, SPE paper # 60766.

Welling, R.W.F., Marketz, F., Moosa, R., Riyami, N., Follows, E.J., de Bruijn, G., Hosny, K., 2007. Inflow profile control in horizontal wells in a fractured carbonate using swellable elastomers. In: 15th SPE Middle East Oil and Gas Show and Conference, Bahrain, SPE paper # 105709.